Characterization of a P-glycoprotein drug transporter from *Toxocara canis* with a novel pharmacological profile

Jeba R.J. Jesudoss Chelladurai [a,b], Douglas E. Jones [a], Matthew T. Brewer [a,*]

[a] *Department of Veterinary Pathology, Iowa State University College of Veterinary Medicine, USA*
[b] *Department of Diagnostic Medicine/ Pathobiology, Kansas State University College of Veterinary Medicine, USA*

ARTICLE INFO

ABSTRACT

P-glycoproteins from the ATP-binding cassette transporter family are responsible for drug evasion by bacterial pathogens and neoplastic cells. More recently, these multidrug resistance transporters have been investigated for contributions to drug resistance in nematode parasites. In this study, we cloned and characterized the P-glycoprotein *Tca-Pgp-11.1* from *Toxocara canis*, the canine intestinal ascarid. Large numbers of *Tca-Pgp-11* transcripts were observed in the intestine of adult male and female worms. Heterologous expression studies confirmed sensitivity to known P-glycoprotein inhibitors. Interestingly, the competitive inhibitor verapamil had lower IC_{50} values than newer generation inhibitors that are designed to allosterically modulate mammalian P-glycoprotein. Consistent with other nematode P-glycoproteins, *Tca-Pgp-11.1* was sensitive to ivermectin and selamectin but not moxidectin. Taken together, our data suggests that *T. canis* P-glycoproteins represent nematode-specific drug targets that could be exploited to enhance efficacy of existing anthelmintics.

1. Introduction

Toxocara canis is an ascarid nematode that infects dogs throughout the world. Adult parasites live within the lumen of the small intestine where they cause vomiting, ill thrift, and a pot-bellied appearance. *T. canis* is also an important zoonosis, causing visceral larva migrans in humans following ingestion of larvated eggs (Glickman and Shofer, 1987).

One reason that *T. canis* is ubiquitous in puppies is that larvae are reactivated in the somatic tissue of bitches and transmitted via the umbilical cord (Burke and Roberson, 1985a, b). Many of these larvae undergo a liver-lung-tracheal migration before maturing to adults in the small intestine. On the other hand, a proportion of larvae undergo somatic migration and become arrested somatic larvae in muscle, kidney, liver, or the heart (Greve, 1971; Schnieder et al., 2011). Larval pools in the tissues of the bitch serve as a reservoir of infection for to up to three litters (Schnieder et al., 2011).

The adults of *T. canis* are typically susceptible to macrocyclic lactones (MLs); several products containing ivermectin and moxidectin are currently available in the United States (Nolan and Lok, 2012). Inhibiting tranmission of reactivated larvae using these macrocyclic lactones has also been achieved (Kramer et al., 2006; Payne and Ridley, 1999).

On the other hand, non-reactivated larvae are not cleared by ML treatment, thus, *T. canis* has some ability to tolerate drug treatment (Clark et al., 1992; Heredia Cardenas et al., 2017; Reinemeyer et al., 1995). In addition to *T. canis* somatic larvae, anthelmintic resistance has also been observed in related ascarids such as *Parascaris* and *Ascaridia* (Collins et al., 2019; Janssen et al., 2013b).

P-glycoproteins (P-gps) are members of the ATP-binding cassette transporter superfamily that actively efflux xenobiotics from cells. For example, P-glycoprotein is well known to expel drugs away from target sites in neoplastic tissues (Bellamy, 1996). In nematodes, there is a repertoire of P-gp genes expressed and several paralogs have been studied in the context of anthelmintic resistance (Figueiredo et al., 2018; Gerhard et al., 2020). Specifically, *Pgp-11* appears associated with drug resistance in parasitic nematodes of veterinary importance and its role has been studied in *Parascaris* (Janssen et al., 2013a, 2015), *Dirofilaria immitis* (Mani et al., 2016), *Haemonchus contortus* (Issouf et al., 2014; Whittaker et al., 2017) and *Cooperia oncophora* (De Graef et al., 2013). *T. canis* expresses a repertoire of P-gps which are currently a subject of investigation in our laboratory (Jesudoss Chelladurai and Brewer, 2019b). We hypothesize that P-glycoproteins of *T. canis* contribute to drug tolerance and exhibit unique pharmacological profiles compared to mammalian P-glycoprotein (MDR1). In this study, we identified

---

Tca-Pgp-11.1 by cloning and bioinformatic analysis. Herein, we investigated the pharmacology of this P-gp using heterologous expression assays and tissue-specific expression using chromogenic *in situ* hybridization.

2. Methods

2.1. Parasites and cDNA library construction

Institutional ethical approval for this study was granted under Iowa State University Protocol 18–1789. Adult *T. canis* male and female worms (pools of 3–5 individuals) were obtained opportunistically from naturally infected dogs and eggs were obtained from gravid females. Parasites were homogenized in Trizol reagent (Life Technologies) and pooled, followed by purification using the Direct-zol RNA Miniprep kit (Zymo Research) according to the manufacturer's instructions. RNA was eluted into 50 μL of nuclease free water, quantified using a Nanodrop1000 spectrophotometer, and stored at −80 °C. RNA quality was assessed using the 260/280 ratio and by electrophoresis in a denaturing bleach agarose gel (Aranda et al., 2012). Synthesis of first-strand cDNA was carried out using 0.5 μg of total RNA, 200 U of SuperScript IV Reverse Transcriptase (Invitrogen) and 2.5 μM Oligo d(T)20 primers, using the manufacturer's recommended protocol.

2.2. Molecular cloning of Tca-Pgp-11.1

We identified the *Tca-Pgp-11* nucleotide sequence on the *T. canis* draft genome assembly Scaffold1303 (Accession number JPKZ01003065.1) on NCBI GenBank. The cDNA of *Tca-Pgp-11.1* was amplified in PCR reactions consisting of 1x OneTaq HotStart DNA polymerase master mix (New England BioLabs), 1 μM of each primer (Pgp11F-HindIII 5′- ACT GAA AAC CCC TTT TGG GGA AGC TTG CCG CCA CCA TGG ATG ACA ATC GCA AGG ACT C -3′ and Pgp11R- BamHI 5′- ACT GAA AAC CCC TTT TGG GGG GAT CCT TAA TGG TGA TGG TGA TGG TGG CTG CGC AGA TCC TGT TTG CGT ATG AGT TCG GCG TAT -3′) and 2 μL of first strand synthesized cDNA in accordance with manufacturer's recommendation. A touch down PCR strategy entailed initial denaturation at 94 °C for 2 min, followed by 20 cycles of cyclic denaturation at 94 °C 15 s, annealing at 65 °C for 15 s with a drop of 1 °C per cycle, cyclic extension at 68 °C for 6 min, and again followed by 20 cycles of cyclic denaturation at 94 °C 15 s, annealing at 45 °C for 15 s, cyclic extension at 68 °C for 6 min and final extension at 68 °C for 10 min. PCR products were purified using Wizard SV Gel and PCR Clean-Up system (Promega), cloned into pCR-XL-TOPO, and transformed into OneShot TOP10 Chemically competent *E. coli* (Life Technologies). Overlapping fragments of *Tca-Pgp-11* were spliced using Gibson assembly and the full-length ORF was cloned into the pCR-XL-TOPO vector for sequencing. Phylogenetic analysis (see Section 2.3) in subsequent steps designated the expressed gene as *Tca-Pgp11.1*. Transformants were analyzed by PCR and sequenced using a primer walking strategy on an Applied Biosystems 3730xl DNA analyzer at the Iowa State University DNA Facility.

2.3. Bioinformatic analyses

Sequences were assembled using GeneStudio Professional Edition version 2.2.0.0 and conceptually translated to the corresponding peptide sequence using EMBOSS Transeq (Rice et al., 2000). The BLAST suite was used to align and confirm sequence identities of nucleotide and translated peptide sequences by comparison to draft *T. canis* genomes WGS: JPKZ01, LYYD01 and UYWY01 (NCBI Genome database assemblies GCA_000803305.1, GCA_001680135.1, and GCA_900622545.1 respectively) (Johnson et al., 2008). The 1282 amino acid long conceptually translated protein sequence was analyzed with ScanProsite (de Castro et al., 2006) and InterPro for residue annotation (Mitchell et al., 2019). Protein secondary structure was predicted using Protter 1.0

(Omasits et al., 2014; Torrisi et al., 2019). Protein tertiary structure was predicted using ModWeb using the combined sequence-profile and PSI-BLAST fold assignment methods (Pieper et al., 2014). Multiple sequence alignments of nucleotide and translated protein sequences were visualized with Multalin version 5.4.1 (Corpet, 1988).

Translated protein sequence of other nematode Pgp sequences were obtained from NCBI GenBank protein database, aligned using MAFFT (Katoh and Standley, 2013). Substitution model was selected using the SMS tool with Bayesian Information Criteria (Lefort et al., 2017). The model with lowest BIC value was LG + F + I + G with 4 parameter gamma distribution (Le and Gascuel, 2008) and maximum likelihood phylogenetic analyses performed using PhyML3.0 (Guindon et al., 2010). The tree was visualized using Mega X (Kumar et al., 2018).

2.4. Heterologous expression in LLC-PK1 cells

A full-length clone of *Tca-Pgp-11.1* was directionally sub-cloned into pcDNA3.1+ mammalian expression vector (Invitrogen) using the HindIII and BamHI restriction sites. Transformants were analyzed by restriction digestion and sequenced by primer walking.

Heterologous expression was conducted in LLC-PK1 cells as described previously (Dupuy et al., 2010b; Godoy et al., 2016). Cells were maintained in Medium 199 containing 10% heat-inactivated fetal bovine serum at 37 °C with 5% CO$_2$. Chemical transfection was carried out using Lipofectamine 2000 according to the manufacturer's instructions; cells were transfected with 5 μg of expression vector at 90% confluency in 24 well plates. Transfectants were held under G418 selection (400 μg/mL) for 2 weeks and remaining cells were transferred to 75 cm^2 cell culture flasks. Transfected cells were used for downstream assays within the first 6 passages.

Expression of *Tca-Pgp-11.1* was verified by qPCR and immunoblotting. Cells were released from culture flasks using 0.25% Trypsin-EDTA. RNA was extracted using the Trizol reagent (Life techonologies) and Direct-zol RNA kit with DNase digestion (ZymoResearch) and quantified using a nanodrop spectrophotometer. Synthesis of first strand cDNA was carried out using iScript Select cDNA synthesis kit (Bio-rad). First strand cDNA diluted 1:10 was used as template for qPCR using the primers listed in Table S1. qPCR was carried out in a StepOne Real-time PCR system (Applied Biosystems) using the Sso Advanced Universal SYBR Green Supermix (Bio-rad). Immunoblots were carried out using 0.5 mg total protein on PVDF membranes. Membranes were probed with primary rabbit polyclonal antibodies (diluted 1:1000 in 1% BSA) targeting the *Tca-Pgp-11* peptide VDAASSKQMKGNAEC (Genscript) (aa 230–244; in ABC transporter integral membrane type-1 fused domain; highlighted in blue in Fig. 1(B)) overnight at 4 °C. Blots were washed three times for 10 min in TBS buffer and then incubated with (1:5000) alkaline phosphatase-labeled mouse anti-rabbit antibodies (Jackson labs) for 2 h at room temperature. Following washing three times with TBS buffer, blots were developed using BCIP solution (Thermo Fisher).

2.5. Efflux inhibition assays

Tca-Pgp-11.1-mediated efflux of known Pgp substrates were measured using a spectrophotometric assay (Dupuy et al., 2010a; Godoy et al., 2015b). *Tca-Pgp-11.1* transfected cells were grown to 90–100% confluency in 24 well plates. Cells were coincubated with P-gp inhibitors in the presence of the fluorescent P-gp substrates Hoechst 33342 (H3342; 1–10 μm) or Rhodamine 123 (R123; 10 μm). For initial kinetic experiments, intracellular R123 accumulation was measured over time in a spectramax plate reader with excitation/emission spectra of 507/529 nm. For H33342 concentration-response experiments, cells were coincubated with dilutions (0.01–1000 μm) of competitive and allosteric P-gp inhibitors, washed in DPBS, and lysed with 0.5% sodium dodecyl sulfate. Fluorescence was recorded using a spectramax plate reader with excitation/emission spectra of 350/461 nm.
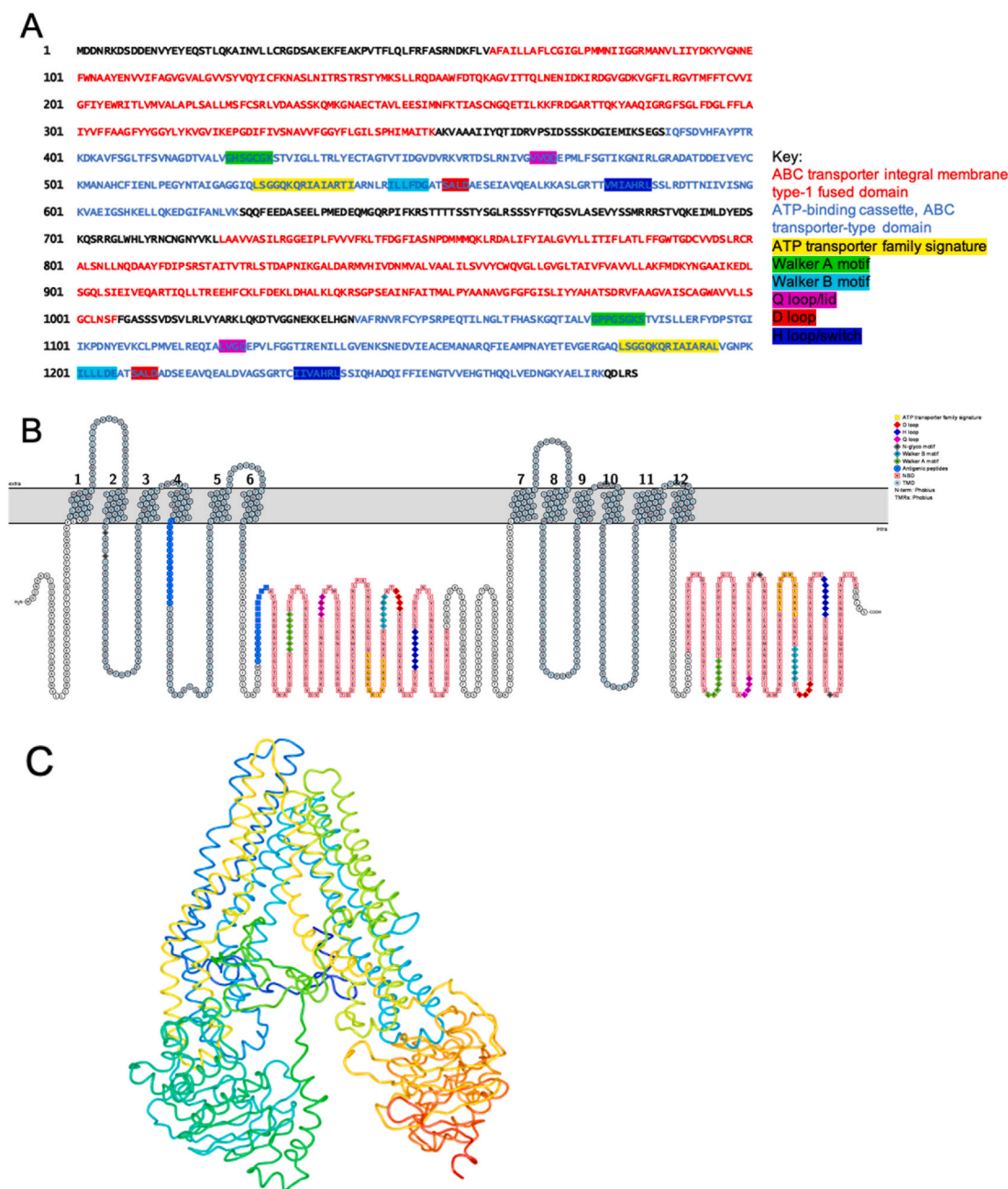
Fig. 1. (A) Primary sequence of *Tca-Pgp-11.1* with motifs predicted by ExPASy ScanProsite. (B) Predicted secondary structure of *Tca-Pgp-11.1* with signature motifs highlighted and transmembrane domains numbered, represented using Protter (C) Tertiary structure of *Tca-Pgp-11.1* modelled after *C. elegans* Pgp-1 crystal structure (protein database accession: 4f4c) using ModWeb.

2.6. Multiple nucleic acid in situ hybridization assay

Parasites were formalin-fixed for 22 h and embedded in paraffin for multiple nucleic acid hybridization studies. Chromogenic *in situ* mRNA hybridization was carried out on 5 μm thick sections according to the protocol optimized for ascarid nematodes (Jesudoss Chelladurai and Brewer, 2019a). Nucleotide probes targeted *Tca-Pgp-11.1*, *T. canis* β-tubulin, and *Bacillus subtilis* DapB (Table S2). Due to the identity of *Tca-Pgp-11.1* and *Tca-Pgp-11.2* (Figure S3) in some of the probe binding regions (MT543030: 421bp −1364 bp), the probes were assumed to be able to bind to both isoforms. Probes were detected using RNAscope 2.5 HD Assay-Red reagents (Advanced Cell Diagnostics) with Fast Red substrate.

2.7. Statistical analysis

Statistical analyses of data were performed using GraphPad Prism version 8. IC_{50} values were calculated using four parameter concentration-response curves. Welch's *t*-test was used when comparing means of individual groups.

3. Results

3.1. Tca-Pgp-11.1 is a P-glycoprotein transporter expressed by Toxocara canis

The cloned full length *Tca-Pgp-11.1* gene was 3849 base pairs, corresponding to a translated protein of 1282 amino acids in length

(GenBank nucleotide accession number: MT543030 and protein accession number: QRN45888). The predicted and the cloned sequences differed at the 5' end; 96 mismatches (~2.6%) in the nucleotide sequences between the predicted and cloned sequences were detected (Supplementary data). Conceptually translated protein and predicted protein sequences showed 97% similarity with the major differences located at the N-terminal end. BLAST analyses revealed the cloned sequence showed 98.88%, 91.88% and 53.84% identity with *T.canis* draft genome-predicted P-gp sequences KHN73709, KHN87227 and KHN89031. The cloned sequence demonstrated 72% identity to *Pgp-11.1* from *Parascaris univalens* (AGL08022), 55% to *Pgp-11* from *Brugia malayi* (CRZ23051) and 55% to *Pgp-11* from *Dirofilaria immitis*

(ALI16773), consistent with similar comparisons in other nematodes (David et al., 2018). Structural bioinformatic analyses of the translated protein sequence showed tandem arrangement of ABC transporter type-1 fused domain and ATP-binding domain in tandem in each half of the protein which is typical of P-glycoproteins (Fig. 1). The ATP transporter family signature motif (LSGGQ) as well as the conserved Walker A, Walker B, Q loop/lid, D loop and H loop/switch motifs were also present. Thus, *Tca-Pgp-11.1* is a P-glycoprotein of the ATP binding cassette transporter family.

Maximum Likelihood phylogenetic analysis of P-gp sequences revealed that *Pgp-11* sequences from *C. elegans* and other parasitic nematodes formed a distinct clade. Spiruroid nematodes such as
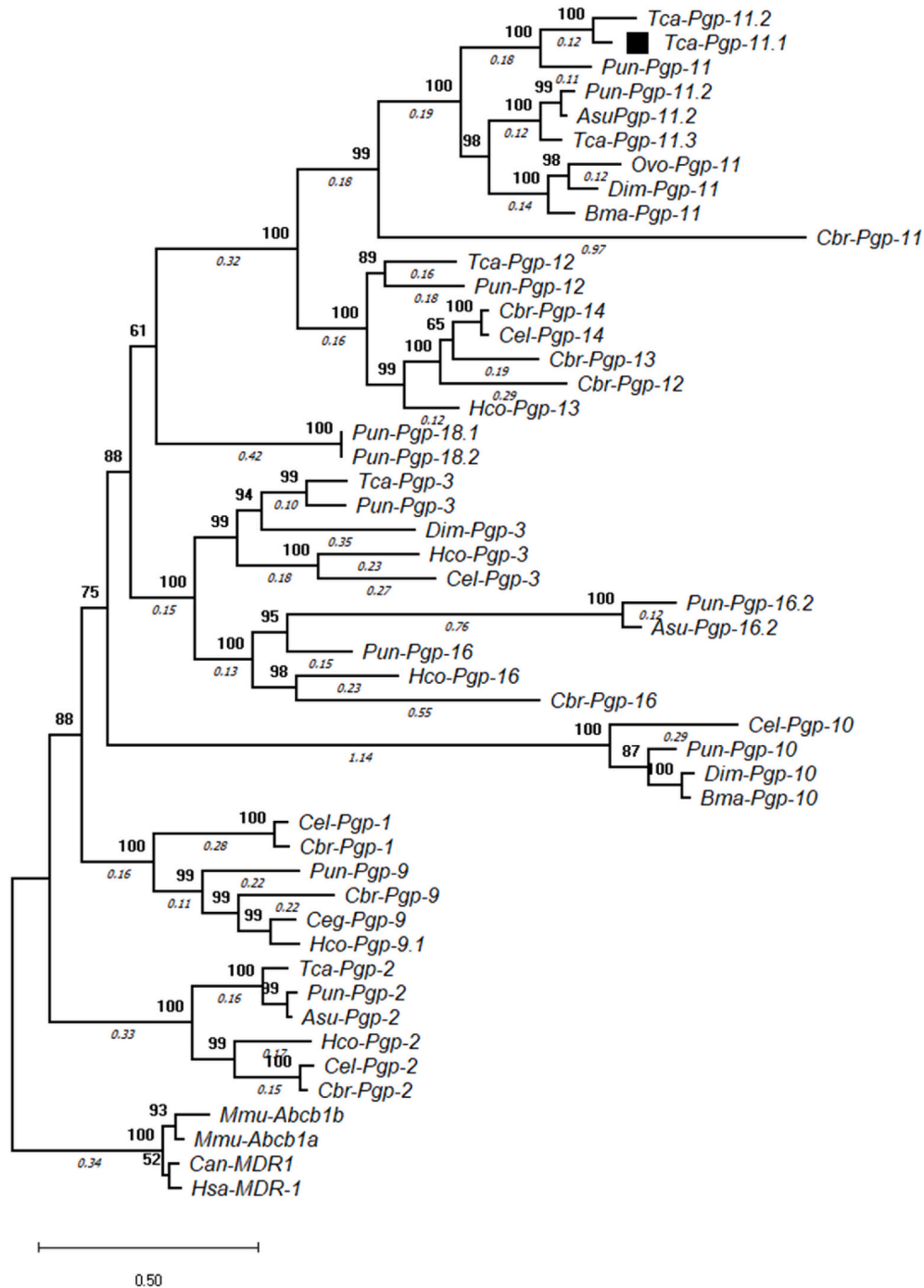

Fig. 2. Maximum likelihood phylogenetic tree of *Tca-Pgp-11.1* (■), predicted *T. canis* and nematode P-gp genes in comparison with those from other nematodes. Mouse, human and dog P-gp (MDR1) protein sequences were used as outgroup. The accession numbers of sequences is listed in Fig S3.

Dirofilaria immitis formed a subclade distinct from *T. canis* and other Ascaridoid nematodes within the *Pgp-11* clade with high statistical support (Fig. 2). Three predicted *T. canis* Pgps were observed in the *Pgp-11* clade – KHN73709, KHN87227 and KHN89031. It is likely that the three are paralogs of *Pgp-11* within the *T. canis* genome.

3.2. Tca-Pgp-11.1 has an unusual pharmacologic inhibition profile

Functional transport assays were conducted by expressing *Tca-Pgp-11.1* in LLC PK1 cells; heterologous expression was confirmed by qPCR and immunoblotting (Fig. 3). *Tca-Pgp-11.1* transcripts were detected for at least 6 passages following transfection (Figure S4). Phenotypically, transfected cells had a significant decrease in H33342 accumulation compared to controls (P < 0.01, Fig. 4), indicating functional efflux activity by *Tca-Pgp-11.1*. Kinetic studies measuring *Tca-Pgp-11.1*-mediated R123 efflux demonstrated that efflux activity plateaued at approximately 50 min (Fig. 5). Even in the presence of 10 μM inhibitor, *Tca-Pgp-11.1* was still capable of H33342 efflux for verapamil, cyclosporine A, loperamide, and tariquidar. Interestingly, inhibitors tacrolimus and reserpine enhanced release of H33342 from non-transfected cells, possibly through a P-gp-independent mechanism.

Known P-gp inhibitors and macrocyclic lactones varied in their ability to block H33342 efflux by *Tca-Pgp-11.1* (Fig. 6, Table 1). Verapamil and valspodar were potent inhibitors of *Tca-Pgp-11.1* with IC$_{50}$ values of approximately 3 μM. Tariquidar, a third generation inhibitor had an IC$_{50}$ value of 68, but with a wide confidence interval that overlapped with verapamil and tariquidar. Future refinement of the expression system with a total removal of the MDR1 background may help detect differences among these different generation inhibitors. Ivermectin and selamectin, competitive inhibitors of P-gp, had IC$_{50}$ values approaching the millimolar range. Moxidectin did not generate a
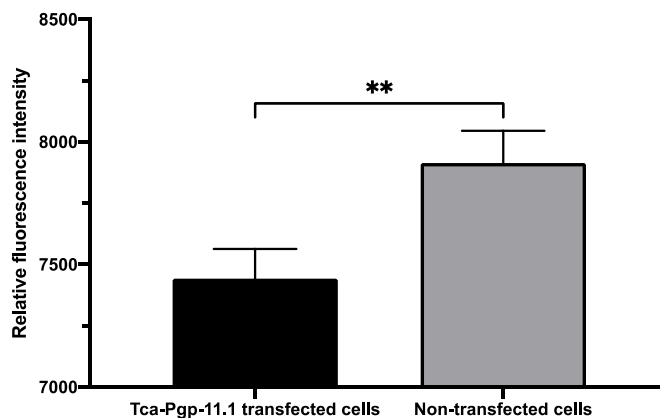

Fig. 4. *Tca-Pgp-11.1*-mediated efflux of Hoechst 33342. Values represent the accumulation of mean and S.E. of 25 independent biological replicates with two technical replicates each. Welch's *t*-test (P < 0.01).

sigmoid concentration-response curve and was not a clear inhibitor of *Tca-Pgp-11*, which was consistent with other nematode P-gps (David et al., 2016, 2018; Godoy et al., 2015a, 2015c; Kaschny et al., 2015; Lloberas et al., 2013).

3.3. Tissue specific expression of Tca-Pgp-11

Multiple nucleic acid hybridization was used to visualize individual mRNA transcripts in tissues of adult male and female worms (Fig. 7). Red-pink spots indicating *Tca-Pgp-11* mRNA transcripts were the most obvious in the columnar cells of the intestine. Expression could also be observed in the hypodermis, but not in the cuticle. Fewer transcripts could be seen in the lateral cords and nerve cords. No *Tca-Pgp-11* mRNA was visualized from male or female reproductive tracts at any transverse section. Positive control for the assay was a β-tubulin component encoded by the *ttb4* gene in *T. canis* which is expressed throughout the worm (Figure S1). On the other hand no signal was detected in any tissue for the negative control *Bacillus subtilis* DapB (Figure S2).

4. Discussion

Anthelmintic resistance is an increasing problem in a wide variety of nematodes. One hypothesis is that P-gps contribute to multi-drug resistance by effluxing drugs away from their molecular targets. P-gps are members of the are ATP-binding cassette cassette class B1 family. Typically, only one or two isoforms of the ABCB1 gene are expressed in mammals. In contrast, nematodes have a repertoire of 10–15 P-gps (Gerhard et al., 2020). The collection of P-gps expressed by *T. canis* is currently being evaluated by our laboratory. One nematode P-gp in particular, *Pgp-11*, has been characterized in a number of parasitic nematodes. In this study, we characterized *Tca-Pgp-11.1*, an ortholog of *Pgp-11* described in *Dirofilaria immitis* (Mani et al., 2016) and *Pgp-11.1* in *Parascaris univalens* (Gerhard et al., 2020) which is expressed by *T. canis*.

The full-length cDNA of *Tca-Pgp-11.1* allowed the prediction of a protein of 1282 amino acid protein. The protein has 2 transmembrane and 2 nucleotide binding domains which are characteristic of the ABCB subfamily. The nucleotide binding domain possessed the characteristic ATP signature motifs, Walker A, Walker B and Q-loop motifs. The two transmembrane domains each contain 6 helices which are possible sites for drug binding. Phylogenetic analysis confirmed that the cloned sequence is an ortholog of *Pgp-11* and was designated *Tca-Pgp-11.1* in accordance with gene naming conventions (Beech et al., 2010). Two other protein sequences encoded in the *T. canis* draft genome were found in the *Pgp-11* clade. These could be paralogs or isoforms of *Pgp-11* due gene duplications, which has been observed with *Pun-Pgp-11* from
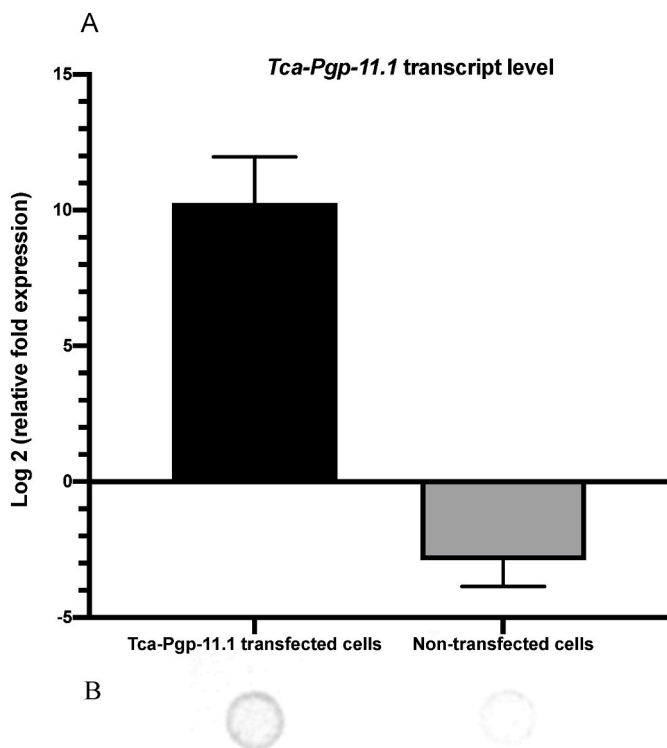

Fig. 3. A) Transcript levels of *Tca-Pgp-11.1*-transfected and non-transfected LLC-PK1 cells. Relative expression over mock-transfected cells was calculated using qPCR with pig *GAPDH* as housekeeping gene. B) Immunoblot of cell lysates (corresponding with bars in panel A) demonstrating reactivity with anti-*Tca-Pgp-11.1* antibody.
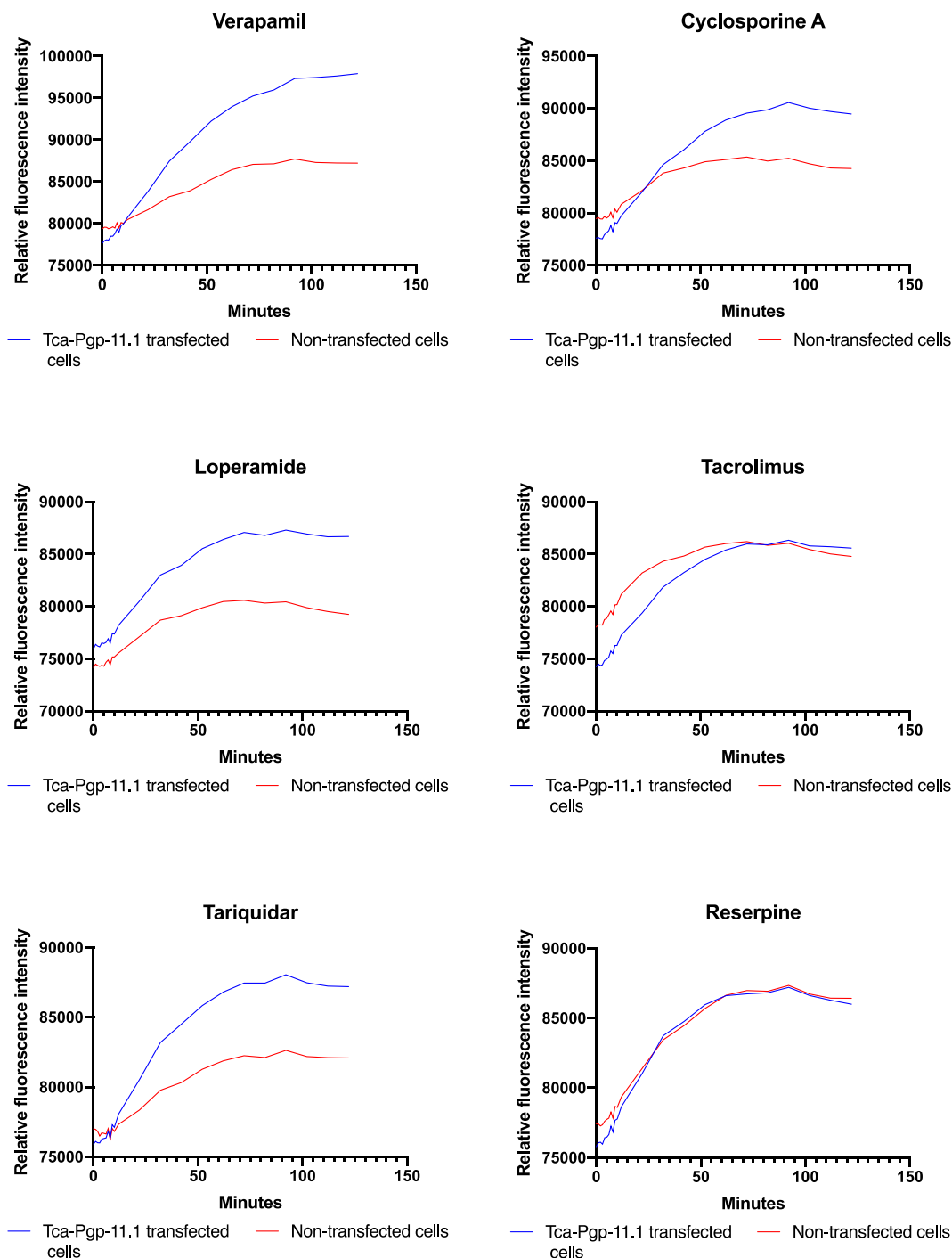
Fig. 5. Kinetics of *Tca-Pgp-11*-mediated efflux of R123 in the presence (10 μM) P-gp inhibitors.

Parascaris (Gerhard et al., 2020).

Functional studies were performed to measure efflux activity of *Tca-Pgp-11.1* and possible inhibition with known P-gp inhibitors. In this study, we expressed the clone represented in mRNA pools from parasites and did not make codon optimization changes. Efflux of the fluorescent substrate H3342 was evident in transfected cells, allowing for the construction of concentration-response curves. In this system, we observed IC_{50} values in the micromolar range. *Tca-Pgp-11.1* was the most sensitive to verapamil, a first generation competitive inhibitor, while it was less sensitive to the third generation P-gp inhibitor tariquidar. Tariquidar binds allosterically to mammalian P-gp and is one of the most potent

inhibitors of mammalian ABCB1 (Loo and Clarke, 2015). Thus, this finding is interesting because it suggests that the corresponding allosteric site on the nematode P-gp could be targeted while sparing the mammalian host. Alternatively, the tariquidar binding site could be absent in the nematode protein. Further development of heterologous expression assays used to study helminth P-gps is needed to fully explore differential pharmacology that could lead to discovered of nematode-specific drugs.

P-gp-mediated drug efflux is hypothesized to contribute to resistance by sequestering anthelmintics away from target receptors. The target of macrocyclic lactones, glutamate-gated chloride channels, are located in
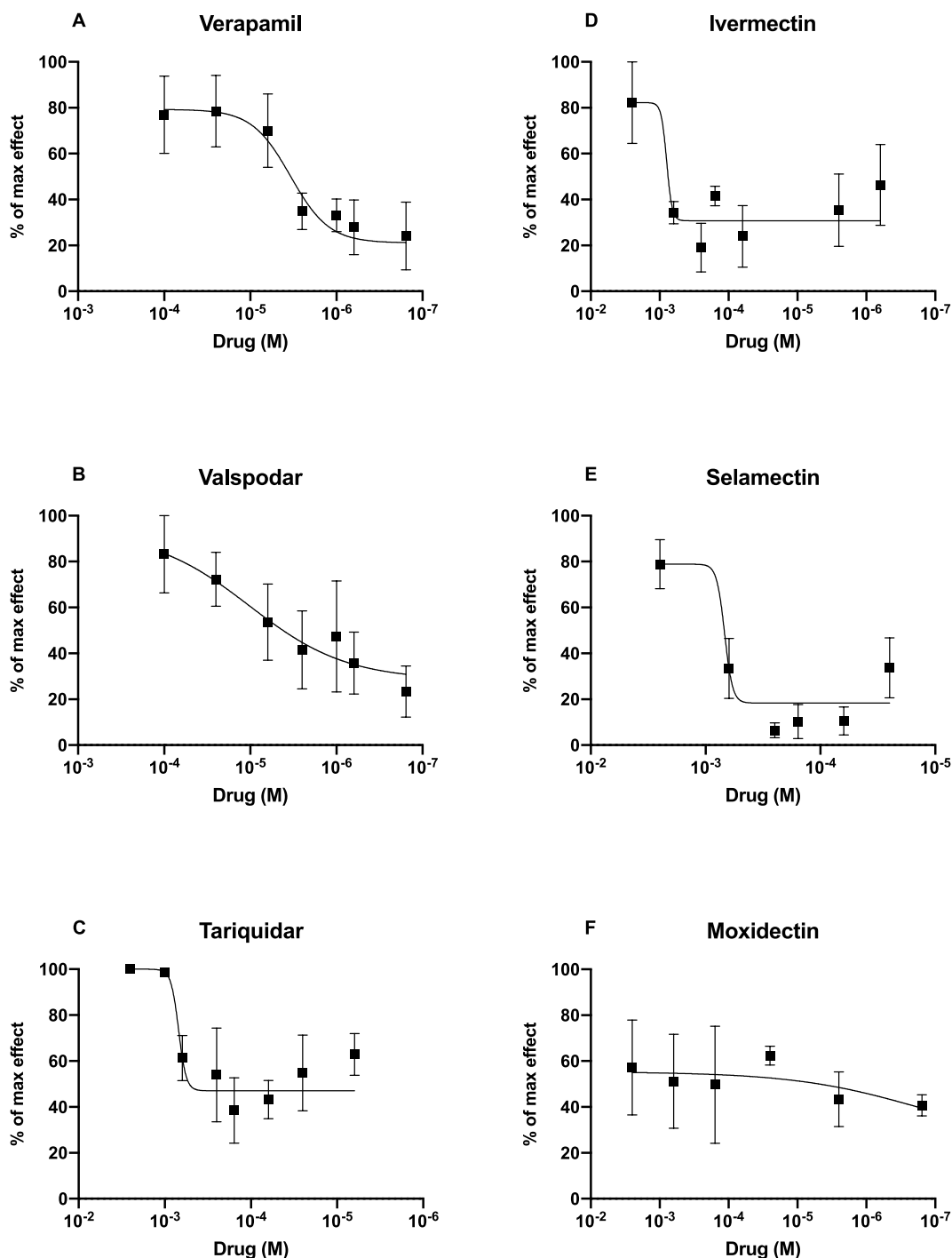
Fig. 6. Inhibition of *Tca-Pgp-11*.1 by P-gp inhibitors (A, B and C) and macrocyclic lactones (D, E and F). Values represent mean and S.E. of three independent experiments with two technical replicates each. Calculated IC$_{50}$ values are given in Table 1.

Table 1

IC$_{50}$ (μM) values for P-glycoprotein inhibitors and macrocyclic lactones for the inhibition of *Tca-Pgp-11.1* as measured by H3342 efflux assays.

Drugs	IC$_{50}$	95% CI
Verapamil	3.32 μM	1.16 μM – 10.37 μM
Valspodar	3.01 μM	0.43 μM – 21.75 μM
Tariquidar	68.46 μM	4.13 μM–217.9 μM
Ivermectin	321.5 μM	282.7 μM–805.1 μM
Selamectin	1024.5 μM	551.8 μM – 3173 μM
Moxidectin	Not Determined	Not Determined

the neurons and reproductive system of nematodes (Li et al., 2014). Using a highly specific *in situ* hybridization technique adapted to ascarids (Jesudoss Chelladurai and Brewer, 2019a), we visualized individual transcripts of *Tca-Pgp-11*. Our probes were unable to differentiate between isoforms *Tca-Pgp-11.1* and *Tca-Pgp-11.2* due to a high level of identity. Our study demonstrates that *Tca-Pgp-11* was expressed at high levels in the intestine, which is similar to patterns of *Peq-Pgp-11* expression observed in adult *Parascaris* (Jesudoss Chelladurai and Brewer, 2019a). We observed few transcripts in the body wall, nerve cord, and lateral cords. There was no expression observed in the reproductive tissues of either sex, which is in contrast to *Peq-Pgp-11*
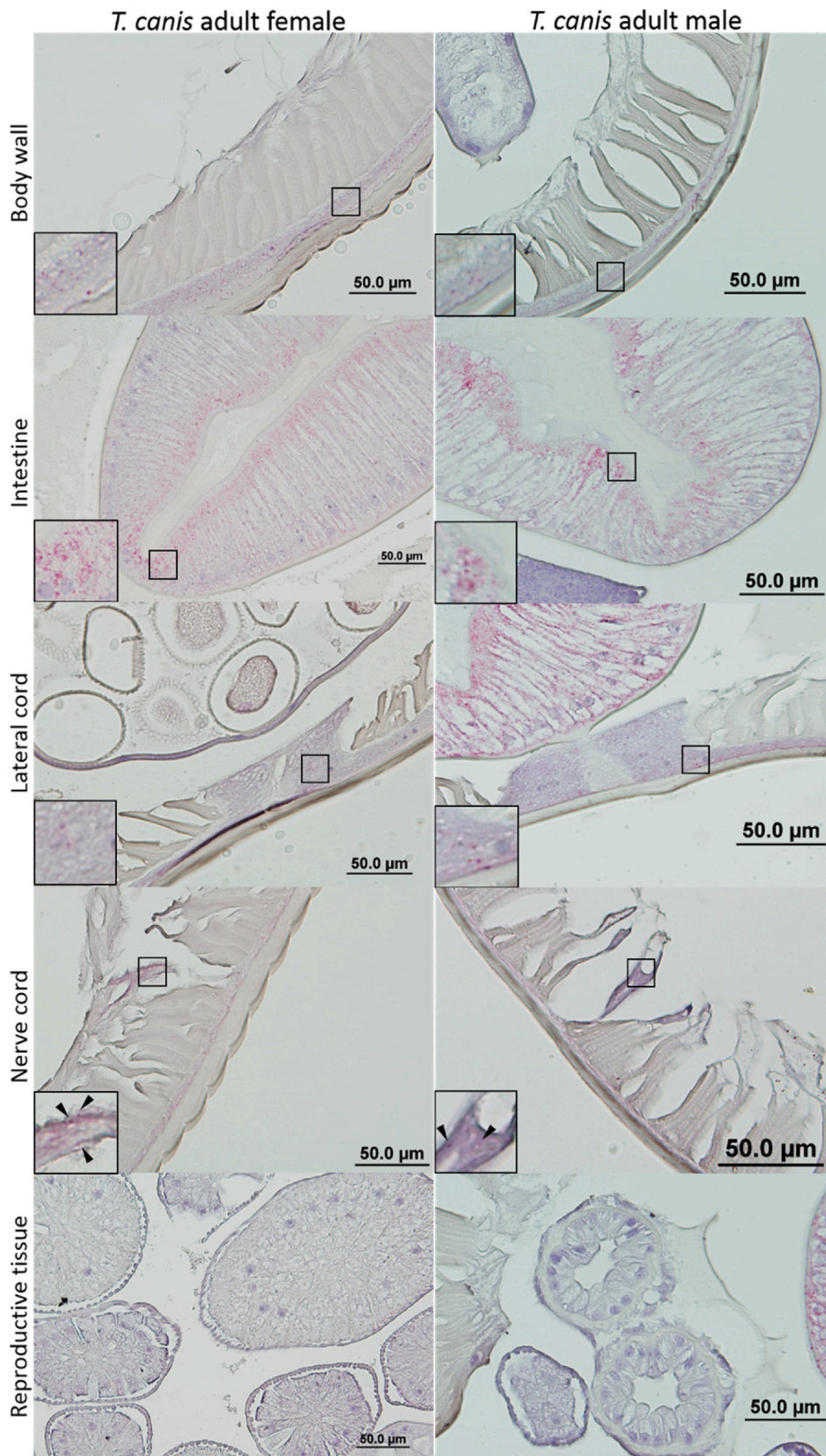
Fig. 7. Detection of *Tc-Pgp-11* transcripts by multiple nucleic acid *in situ* hybridization in adult female and male *Toxocara canis*. Positive signal resulting from hybridization of *Tca-Pgp-11* probes to isoforms 11.1 and 11.2 appear as red punctate dots. Black boxes indicate the location of high magnification insets. Black arrows point to red dots in locations with low signal. (For interpretation of the references to colour in this figure legend, the reader is referred to the Web version of this article.)

which was expressed in the reproductive tissues of both sexes. Thus, it appears that the ascarid intestine is an important site for P-gp activity and possibly regulating the entry of xenobiotics into parasite tissues. In mammals, P-gp are present within intestinal epithelial cells where they are a barrier to absorption of oral medications (Benet et al., 1999). Studies investigating functional efflux of anthelmintics by helminth gut cells may shed additional light on how nematode P-gp prevents anthelmintics from arriving at their target site.

In this study, we described the structure and tissue distribution of

Tca-Pgp-11, a P-gp from *T. canis*. Functional studies demonstrated alternative inhibition profiles, suggesting a unique pharmacology that could be amenable to exploitation. Future studies investigating unique regions of parasite P-gps are needed to expose possible nematode-specific drug binding sites. Such discoveries could lead the way to combination therapies whereby inhibition of P-gp enhances performance of existing anthelmintic drugs.
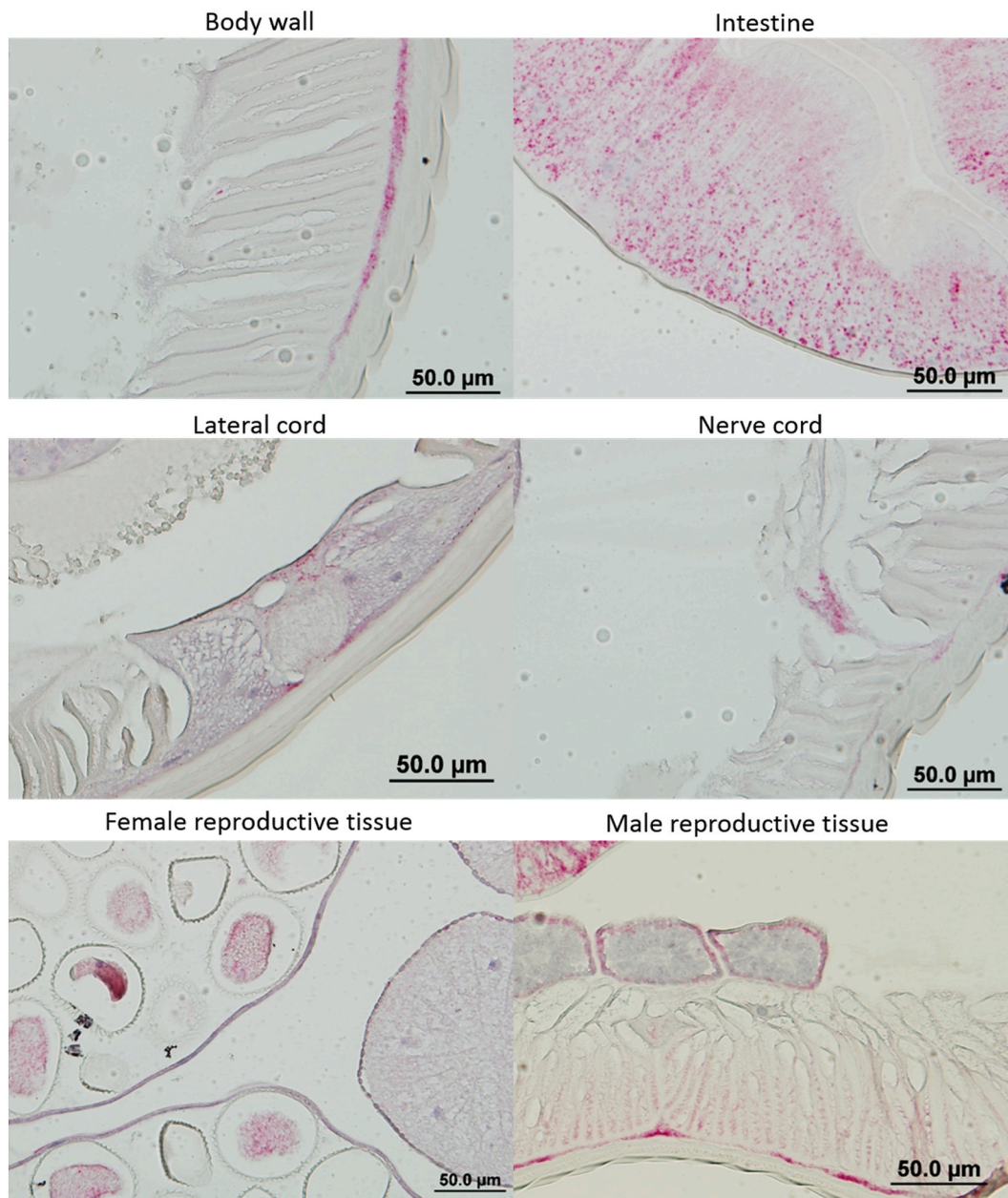

Fig. S1. Nucleic acid hybridization signal resulting from hybridization of positive control probes targeting *T. canis* tubulin gene *ttb4*.

Fig. S2. Absence of hybridization signal with negative control probe targeting *B. subtilis* DapB gene. No positive signal appeared in either sex.
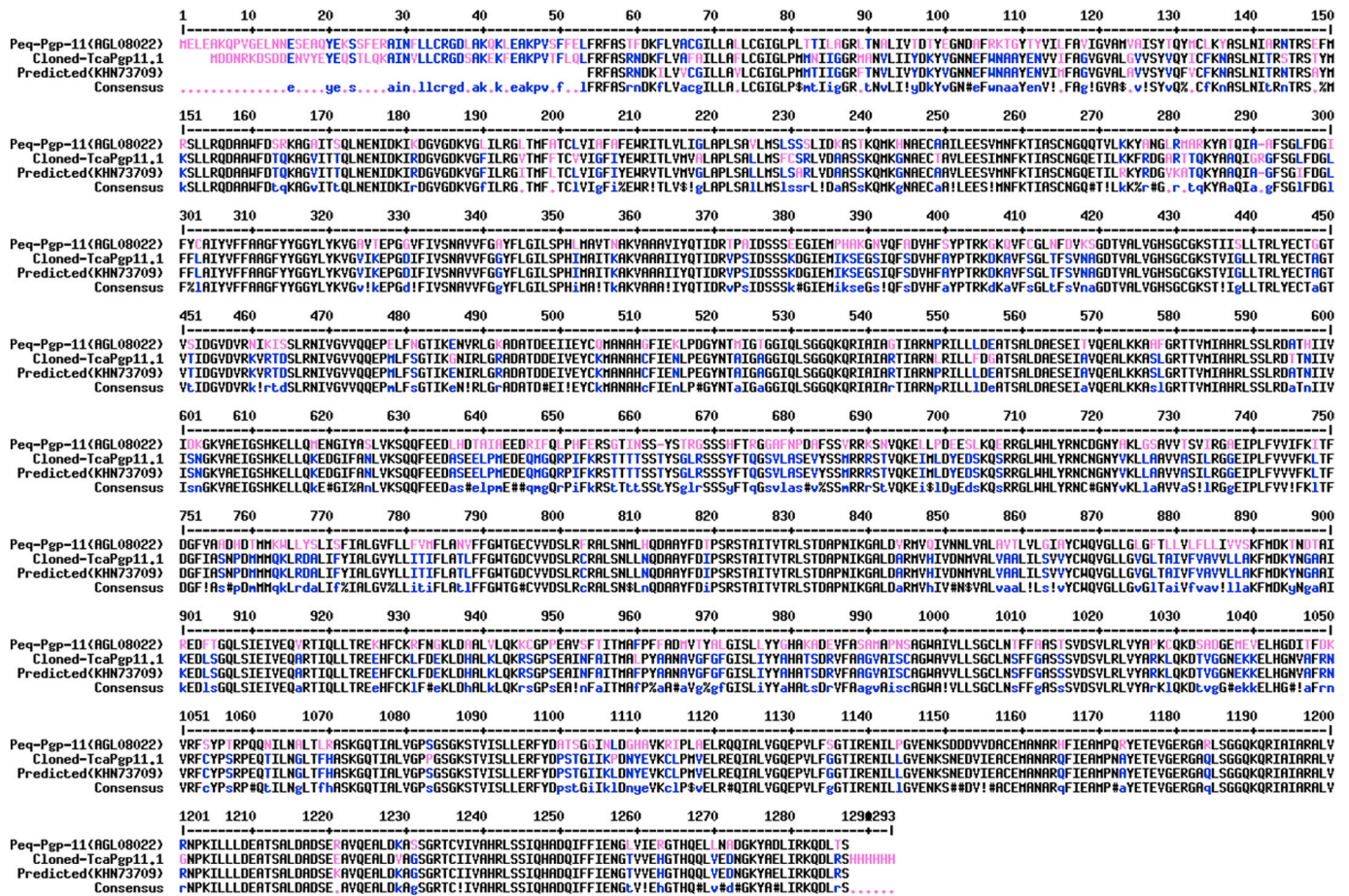
Fig. S3. Multiple sequence alignments of cloned *Tca-Pgp-11.1* (MT543030.1), *Tca-Pgp-11.2* sequence (JPKZ01000445.1) and *Tca-Pgp-11.3* (JPKZ01000091.1). Alignments were created using Multalign. High consensus and no substitution sites are shown in black. Low consensus and substitution sites are shown in red.
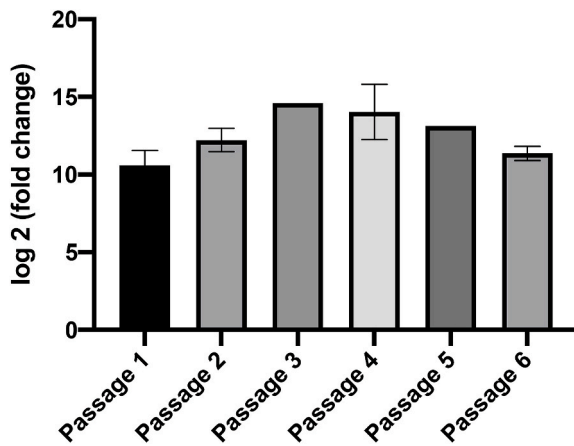

Fig. S4. Stable expression of *Tca-Pgp-11.1* in LLC-PK1 cells. Relative expression over non-transfected cells was calculated using qPCR with pig *GAPDH* as housekeeping gene. Error bars represent standard error. Each passage had two technical replicates and 1 to 3 biological replicates.

Table S1
Primers used in qPCR

qTcPg-1F	CGCAAGCAGCAAGCAAATGA
qTcPg-1R	GAGAAGCCGGCAATTTGTGC
PK1GapDHF	AACTGCTTGGCACCCCTGGC
PK1GapDHR	TTGGCAGCGCCGGTAGAAGC
PK1mdr1F	GCCATGGCAGTGGGACAGGT
PK1mdr1R	AAGCCCACGGTGCTGTAGCTG

Table S2
Probes used in Chromogenic *in situ* mRNA hybridization

Probe	GenBank Accession numbers	Target nucleotides
Toxocara canis Pgp-11.1	MT543030	421–1364
Toxocara canis β-tubulin	JPKZ01000754.1:68516-75076	4–1004
Bacillus subtilis dapB	EF191515	414–862

Declaration of competing interest

The authors have no conflicts of interest to report, financial or otherwise.

Acknowledgements

References

Aranda, P.S., LaJoie, D.M., Jorcyk, C.L., 2012. Bleach gel: a simple agarose gel for analyzing RNA quality. Electrophoresis 33, 366–369.

Beech, R.N., Wolstenholme, A.J., Neveu, C., Dent, J.A., 2010. Nematode parasite genes: what's in a name? Trends Parasitol. 26, 334–340.

Bellamy, W.T., 1996. P-glycoproteins and multidrug resistance. Annu. Rev. Pharmacol. Toxicol. 36, 161–183.

Benet, L.Z., Izumi, T., Zhang, Y.C., Silverman, J.A., Wacher, V.J., 1999. Intestinal MDR transport proteins and P-450 enzymes as barriers to oral drug delivery. J. Contr. Release 62, 25–31.

Burke, T.M., Roberson, E.L., 1985a. Prenatal and lactational transmission of Toxocara canis and Ancylostoma caninum: experimental infection of the bitch at midpregnancy and at parturition. Int. J. Parasitol. 15, 485–490.

Burke, T.M., Roberson, E.L., 1985b. Prenatal and lactational transmission of Toxocara canis and Ancylostoma caninum: experimental infection of the bitch before pregnancy. Int. J. Parasitol. 15, 71–75.

Clark, J.N., Daurio, C.P., Plue, R.E., Wallace, D.H., Longhofer, S.L., 1992. Efficacy of ivermectin and pyrantel pamoate combined in a chewable formulation against heartworm, hookworm, and ascarid infections in dogs. Am. J. Vet. Res. 53, 517–520.

Collins, J.B., Jordan, B., Baldwin, L., Hebron, C., Paras, K., Vidyashankar, A.N., Kaplan, R.M., 2019. Resistance to fenbendazole in Ascaridia dissimilis, an important nematode parasite of turkeys. Poultry Sci. 98, 5412–5415.

Corpet, F., 1988. Multiple sequence alignment with hierarchical clustering. Nucleic Acids Res. 16, 10881–10890.

David, M., Lebrun, C., Duguet, T., Talmont, F., Beech, R., Orlowski, S., André, F., Prichard, R.K., Lespine, A., 2018. Structural model, functional modulation by ivermectin and tissue localization of Haemonchus contortus P-glycoprotein-13. Int J Parasitol Drugs Drug Resist 8, 145–157.

David, M.A., Orlowski, S., Prichard, R.K., Hashem, S., André, F., Lespine, A., 2016. In silico analysis of the binding of anthelmintics to Caenorhabditis elegansP-glycoprotein 1. Int J Parasitol Drugs Drug Resist 6, 299–313.

de Castro, E., Sigrist, C.J., Gattiker, A., Bulliard, V., Langendijk-Genevaux, P.S., Gasteiger, E., Bairoch, A., Hulo, N., 2006. ScanProsite: detection of PROSITE signature matches and ProRule-associated functional and structural residues in proteins. Nucleic Acids Res. 34, W362–365.

De Graef, J., Demeler, J., Skuce, P., Mitreva, M., Von Samson-Himmelstjerna, G., Vercruysse, J., Claerebout, E., Geldhof, P., 2013. Gene expression analysis of ABC transporters in a resistant Cooperia oncophora isolate following in vivo and in vitro exposure to macrocyclic lactones. Parasitology 140, 499–508.

Dupuy, J., Alvinerie, M., Menez, C., Lespine, A., 2010a. Interaction of anthelmintic drugs with P-glycoprotein in recombinant LLC-PK1-mdr1a cells. Chem. Biol. Interact. 186, 280–286.

Dupuy, J., Alvinerie, M., Ménez, C., Lespine, A., 2010b. Interaction of anthelmintic drugs with P-glycoprotein in recombinant LLC-PK1-mdr1a cells. Chem. Biol. Interact. 186, 280–286.

Figueiredo, L.A., Rebouças, T.F., Ferreira, S.R., Rodrigues-Luiz, G.F., Miranda, R.C., Araujo, R.N., Fujiwara, R.T., 2018. Dominance of P-glycoprotein 12 in phenotypic resistance conversion against ivermectin in Caenorhabditis elegans. PLoS One 13, e0192995.

Gerhard, A.P., Krücken, J., Heitlinger, E., Janssen, I.J.I., Basiaga, M., Kornaś, S., Beier, C., Nielsen, M.K., Davis, R.E., Wang, J., von Samson-Himmelstjerna, G., 2020. The P-glycoprotein repertoire of the equine parasitic nematode Parascaris univalens. Sci. Rep. 10, 13586.

Glickman, L.T., Shofer, F.S., 1987. Zoonotic visceral and ocular larva migrans. Vet Clin North Am Small Anim Pract 17, 39–53.

Godoy, P., Che, H., Beech, R.N., Prichard, R.K., 2015a. Characterization of Haemonchus contortus P-glycoprotein-16 and its interaction with the macrocyclic lactone anthelmintics. Mol. Biochem. Parasitol. 204, 11–15.

Godoy, P., Che, H., Beech, R.N., Prichard, R.K., 2015b. Characterization of Haemonchus contortus P-glycoprotein-16 and its interaction with the macrocyclic lactone anthelmintics. Mol. Biochem. Parasitol. 204, 11–15.

Godoy, P., Che, H., Beech, R.N., Prichard, R.K., 2016. Characterisation of P-glycoprotein-9.1 in Haemonchus contortus. Parasites Vectors 9, 52.

Godoy, P., Lian, J., Beech, R.N., Prichard, R.K., 2015c. Haemonchus contortus P-glycoprotein-2: in situ localisation and characterisation of macrocyclic lactone transport. Int. J. Parasitol. 45, 85–93.

Greve, J.H., 1971. Age resistance to Toxocara canis in ascarid-free dogs. Am. J. Vet. Res. 32, 1185–1192.

Guindon, S., Dufayard, J.F., Lefort, V., Anisimova, M., Hordijk, W., Gascuel, O., 2010. New algorithms and methods to estimate maximum-likelihood phylogenies: assessing the performance of PhyML 3.0. Syst. Biol. 59, 307–321.

Heredia Cardenas, R., Romero Núñez, C., Miranda Contreras, L., 2017. Efficacy of two anthelmintic treatments, spinosad/milbemycin oxime and ivermectin/praziquantel in dogs with natural Toxocara spp. infection. Vet. Parasitol. 247, 77–79.

Issouf, M., Guégnard, F., Koch, C., Le Vern, Y., Blanchard-Letort, A., Che, H., Beech, R.N., Kerboeuf, D., Neveu, C., 2014. Haemonchus contortus P-glycoproteins interact with host eosinophil granules: a novel insight into the role of ABC transporters in host-parasite interaction. PLoS One 9, e87802.

Janssen, I.J., Krücken, J., Demeler, J., Basiaga, M., Kornaś, S., von Samson-Himmelstjerna, G., 2013a. Genetic variants and increased expression of Parascaris equorum P-glycoprotein-11 in populations with decreased ivermectin susceptibility. PLoS One 8, e61635.

Janssen, I.J., Krücken, J., Demeler, J., von Samson-Himmelstjerna, G., 2015. Transgenically expressed Parascaris P-glycoprotein-11 can modulate ivermectin susceptibility in Caenorhabditis elegans. Int J Parasitol Drugs Drug Resist 5, 44–47.

Janssen, I.J.I., Krucken, J., Demeler, J., Basiaga, M., Kornas, S., von Samson-Himmelstjerna, G., 2013b. Genetic variants and increased expression of Parascaris equorum P-glycoprotein-11 in populations with decreased ivermectin susceptibility. PLoS One 8.

Jesudoss Chelladurai, J., Brewer, M.T., 2019a. Detection and quantification of Parascaris P-glycoprotein drug transporter expression with a novel mRNA hybridization technique. Vet. Parasitol. 267, 75–83.

Jesudoss Chelladurai, J.R., Brewer, M.T., 2019b. Exploring the role of ABCB1 transporters in Toxocara canis. World association for the advancement of veterinary parasitology, Madison, WI.

Johnson, M., Zaretskaya, I., Raytselis, Y., Merezhuk, Y., McGinnis, S., Madden, T.L., 2008. NCBI BLAST: a better web interface. Nucleic Acids Res. 36, W5–9.

Kaschny, M., Demeler, J., Janssen, I.J., Kuzmina, T.A., Besognet, B., Kanellos, T., Kerboeuf, D., von Samson-Himmelstjerna, G., Krücken, J., 2015. Macrocyclic lactones differ in interaction with recombinant P-glycoprotein 9 of the parasitic nematode Cylicocylus elongatus and ketoconazole in a yeast growth assay. PLoS Pathog. 11, e1004781.

Katoh, K., Standley, D.M., 2013. MAFFT multiple sequence alignment software version 7: improvements in performance and usability. Mol. Biol. Evol. 30, 772–780.

Kramer, F., Hammerstein, R., Stoye, M., Epe, C., 2006. Investigations into the prevention of prenatal and lactogenic Toxocara canis infections in puppies by application of moxidectin to the pregnant dog. J. Vet. Med. B 53, 218–223.

Kumar, S., Stecher, G., Li, M., Knyaz, C., Tamura, K., 2018. MEGA X: molecular evolutionary genetics analysis across computing platforms. Mol. Biol. Evol. 35, 1547–1549.

Le, S.Q., Gascuel, O., 2008. An improved general amino acid replacement matrix. Mol. Biol. Evol. 25, 1307–1320.

Lefort, V., Longueville, J.E., Gascuel, O., 2017. SMS: smart model selection in PhyML. Mol. Biol. Evol. 34, 2422–2424.

Li, B.W., Rush, A.C., Weil, G.J., 2014. High level expression of a glutamate-gated chloride channel gene in reproductive tissues of Brugia malayi may explain the sterilizing effect of ivermectin on filarial worms. Internet J. Parasit. Dis. 4, 71–76.

Lloberas, M., Alvarez, L., Entrocasso, C., Virkel, G., Ballent, M., Mate, L., Lanusse, C., Lifschitz, A., 2013. Comparative tissue pharmacokinetics and efficacy of moxidectin, abamectin and ivermectin in lambs infected with resistant nematodes: impact of drug treatments on parasite P-glycoprotein expression. Int J Parasitol Drugs Drug Resist 3, 20–27.

Loo, T.W., Clarke, D.M., 2015. Mapping the binding site of the inhibitor tariquidar that stabilizes the first transmembrane domain of P-glycoprotein. J. Biol. Chem. 290, 29389–29401.

Mani, T., Bourguinat, C., Keller, K., Ashraf, S., Blagburn, B., Prichard, R.K., 2016. Interaction of macrocyclic lactones with a Dirofilaria immitis P-glycoprotein. Int. J. Parasitol. 46, 631–640.

Mitchell, A.L., Attwood, T.K., Babbitt, P.C., Blum, M., Bork, P., Bridge, A., Brown, S.D., Chang, H.Y., El-Gebali, S., Fraser, M.I., Gough, J., Haft, D.R., Huang, H., Letunic, I., Lopez, R., Luciani, A., Madeira, F., Marchler-Bauer, A., Mi, H., Natale, D.A., Necci, M., Nuka, G., Orengo, C., Pandurangan, A.P., Paysan-Lafosse, T., Pesseat, S., Potter, S.C., Qureshi, M.A., Rawlings, N.D., Redaschi, N., Richardson, L.J., Rivoire, C., Salazar, G.A., Sangrador-Vegas, A., Sigrist, C.J.A., Sillitoe, I., Sutton, G. G., Thanki, N., Thomas, P.D., Tosatto, S.C.E., Yong, S.Y., Finn, R.D., 2019. InterPro in 2019: improving coverage, classification and access to protein sequence annotations. Nucleic Acids Res. 47, D351–D360.

Nolan, T.J., Lok, J.B., 2012. Macrocyclic lactones in the treatment and control of parasitism in small companion animals. Curr. Pharmaceut. Biotechnol. 13, 1078–1094.

Omasits, U., Ahrens, C.H., Müller, S., Wollscheid, B., 2014. Protter: interactive protein feature visualization and integration with experimental proteomic data. Bioinformatics 30, 884–886.

Payne, P.A., Ridley, R.K., 1999. Strategic use of ivermectin during pregnancy to control Toxocara canis in greyhound puppies. Vet. Parasitol. 85, 305–312.

Pieper, U., Webb, B.M., Dong, G.Q., Schneidman-Duhovny, D., Fan, H., Kim, S.J., Khuri, N., Spill, Y.G., Weinkam, P., Hammel, M., Tainer, J.A., Nilges, M., Sali, A., 2014. ModBase, a database of annotated comparative protein structure models and associated resources. Nucleic Acids Res. 42, D336–D346.

Reinemeyer, C.R., Faulkner, C.T., Assadi-Rad, A.M., Burr, J.H., Patton, S., 1995. Comparison of the efficacies of three heartworm preventives against experimentally induced infections with Ancylostoma caninum and Toxocara canis in pups. J. Am. Vet. Med. Assoc. 206, 1710–1715.

Rice, P., Longden, I., Bleasby, A., 2000. EMBOSS: the European molecular biology open software suite. Trends Genet. 16, 276–277.

Schnieder, T., Laabs, E.M., Welz, C., 2011. Larval development of Toxocara canis in dogs. Vet. Parasitol. 175, 193–206.

Torrisi, M., Kaleel, M., Pollastri, G., 2019. Deeper profiles and cascaded recurrent and convolutional neural networks for state-of-the-art protein secondary structure prediction. Sci. Rep. 9, 12374.

Whittaker, J.H., Carlson, S.A., Jones, D.E., Brewer, M.T., 2017. Molecular mechanisms for anthelmintic resistance in strongyle nematode parasites of veterinary importance. J. Vet. Pharmacol. Therapeut. 40, 105–115.